Article

A new-infrared probe targeting mitochondria via regulation of molecular hydrophobicity

June Sung, Jun Gi Rho, Gyeong G Jeon, Yeonjeong Chu, Jun Sik Min, sanghee Lee, Jong Hyun Kim, Wook Kim, and eunha kim

Bioconjugate Chem., **Just Accepted Manuscript** • DOI: 10.1021/acs.bioconjchem.8b00845 • Publication Date (Web): 18 Dec 2018

Title: A new-infrared probe targeting mitochondria via regulation of molecular hydrophobicity

Authors: June Sung[1,†], Jun Gi Rho[1,†], Gyeong G Jeon[1], Yeonjeong Chu[1,2], Jun Sik Min[3], Sanghee Lee[2], Jong Hyun Kim[1], Wook Kim[1,*], Eunha Kim[1,3*]

Affiliations:

[1]Department of Molecular Science and Technology, Ajou University, Suwon 16499, Korea

[2]Center for Neuro-Medicine, Brain Science Institute, Korea Institute of Science and Technology, Seoul 02792, Korea

[3]Department of Applied Chemistry and Biological Engineering, Ajou University, Suwon 16499, Korea

*Correspondence to: wookkim21@ajou.ac.kr, ehkim01@ajou.ac.kr

[†]These authors equally contributed to this work.

Keywords: Silicon rhodamine, Near-IR probe, Fluorescent probe, mitochondria

Abstract:

Herein, we developed a near-infrared (NIR) fluorescent probe for mitochondrial staining based on the NIR fluorochrome, silicon-rhodamine. The hydrophobicity of the fluorescent core was systematically modified by conjugation with 10 different commercial amines. The resulting fluorescent compounds exhibited similar photophysical properties but diverse hydrophobicity. We identified the optimal level of hydrophobicity associated with high mitochondrial targeting efficiency. In particular, the SiR-Mito 8 probe provided excellent mitochondrial staining and successfully differentiated the live Hep3B cancer cells from normal L02 cells *in vitro*.

Keywords

Mitochondria, fluorescent probes, near-IR, silicon rhodamine

1. Introduction

Mitochondria provide cellular energy by generating adenosine triphosphate (ATP) via oxidative phosphorylation. In addition, they play important roles in cell signaling including modulation of ROS production(*1*), regulation of apoptotic cell death(*2*), and maintenance of redox homeostasis(*3*), innate immunity(*4*) and autophagy(*5*). Consequently, mitochondrial dysfunction results in a number of human conditions ranging from neurodegenerative diseases(*6*) to atherosclerosis(*7*), and diabetes(*8*).

Mitochondria are surrounded by a double-membrane, comprising an inner and an outer membrane, and mitochondrial morphology varies considerably between different cell types. In live cells, mitochondrial morphology is continuously modified by the combined action of fission and fusion events(*9*), crucial to maintain mitochondrial function under cellular stress(*10, 11*). Therefore, the morphology of mitochondria is dependent on the cell function and disease states. Recent studies indicated that mitochondrial morphology can be utilized as a biological marker for the diagnosis of cancer phenotypes and to monitor drug response(*12*). Consequently, there is a high demand for fluorescent mitochondrial bioprobes allowing for the investigation of cell signaling and serving as molecular diagnostic tools.

The large difference in membrane potential (positive in the mitochondrial intermembrane space and negative in the mitochondrial matrix) across the mitochondrial inner membrane can be efficiently exploited for targeting the compounds to mitochondria. Therefore, most fluorescent bioprobes for mitochondria are based on compound conjugation with lipophilic cations (typically triphenyl phosphonium ion)(*13*), allowing for the efficient transfer of molecules through lipid bilayers and their accumulation in the mitochondrial matrix.(*14*) However, systematic studies addressing the effect of hydrophobicity on the efficiency of mitochondrial targeting by specific fluorophores are rarely reported. Therefore, developing fluorescent probes to monitor mitochondrial function can be a difficult task, as it must be preceded by proper optimization. In this context, we reasoned that systematic modification of fluorophore hydrophobicity could provide an excellent guide for future development of efficient and versatile mitochondrial fluorescent probes. In addition, considering the growing interest in mitochondria-specific drug delivery(*15-17*), this strategy would help developing theragnostic chemical tools, especially for diseases involving mitochondria.

Herein, we developed a near-infrared (NIR) fluorescent probe for mitochondrial staining. Specifically, the hydrophobicity of the fluorescent core of a NIR fluorochrome, silicon-rhodamine, was modified by the addition of 10 different commercial amines. The resulting compounds displayed similar photophysical properties, such as excitation wavelength (654 ± 4 nm), emission wavelength (667 ± 1 nm), and quantum yield (0.31 ± 0.05), but diverse cLogP values, ranging from 2.29 to 6.33. By co-staining with a commercial green-fluorescent mitochondrial probe, we found that probe hydrophobicity had a significant impact on the efficiency of mitochondria targeting. Among the tested probes, SiR-Mito 8 exhibited excellent mitochondrial staining. In addition, SiR-Mito 8 successfully distinguished the liver Hep3B cancer cells from normal L02 cells, *in vitro*.

2. Results and discussion

Mitochondria provide cellular energy by utilizing the proton electrochemical gradient potential generated by the respiratory electron transport chain (ETC) across the mitochondrial membrane. Electron transport, occurring at the inner mitochondrial membrane, provides the energy required by pumps to translocate proton ions from the mitochondrial matrix to the intermembrane space (complexes I, III, and IV). Therefore, the most straightforward approach for targeting mitochondria is the generation of lipophilic cations(*14*) allowing for probe accumulation inside the mitochondrial matrix by the electrochemical gradient. To develop a new near-IR mitochondria targeting bioprobe, we selected SiR-Me(*18-20*) as the lipophilic cationic fluorochrome. Since, silicon substitution of the oxygen atom in the rhodamine fluorochrome shifts the emission wavelength of SiR to the NIR range (>680 nm) preserving the small size of the molecule (MW ≈ 470), we reasoned that SiR-Me would be a suitable fluorochrome for a systematic evaluation of the effect of probe hydrophobicity on the efficiency of mitochondria targeting.

Starting with 3-bromoaniline, compound **2** was synthesized by a facile one-pot synthesis process, including lithiation, silylanization and oxidation of compound **1** (**Figure 1**)(*18-21*). The reaction between compound **2** and lithiated compound **3**, followed by acidic deprotection, resulted in the desired SiR-Me compound (compound **4**). Afterward, we conjugated SiR-Me with 10 different commercial amines to generate a library of SiR-Me analogs (SiR-Mito) with various cLogP values, reflecting different hydrophobicity (**Table 1**). The resulting library exhibited a molecular weight range from 470.3 to 554.4 dalton and a cLogP value range from 2.29 to 6.55. We confirmed that conjugation of the different amines by an amide linkage resulted in probes with different hydrophobicity but similar photophysical properties such as excitation (654 ± 4 nm) wavelength, emission (667 ± 1 nm) wavelength and quantum yield (0.31 ± 0.05).

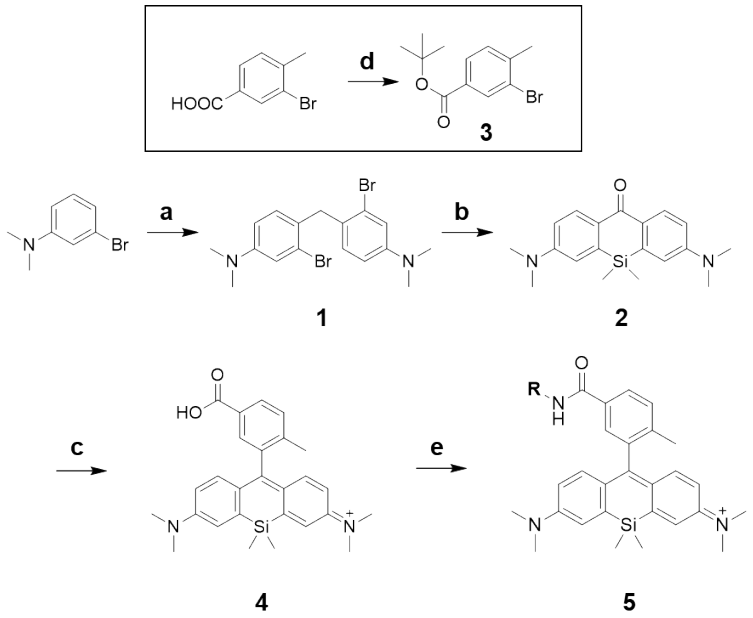

Figure 1. Synthetic scheme for near-infrared (NIR) fluorescent mitochondria probes based on silicon rhodamine core. a) Formaldehyde, AcOH, 60 ºC 1.5 h, b) *sec*-BuLi, $SiCl_2Me_2$, THF, -78 ºC, then $KMnO_4$, acetone, 0 ºC, c) **3**, *tert*-BuLi, THF, -78 ºC, then 6N HCl, 40 ºC d) Di-*tert*-butyl dicarbonate, DMAP, THF, reflux, e) PyBOP, DIPEA, amine analogs, DMF, room temperature

Table 1. Photophysical properties, cLogP value, and correlation coefficient for the colocalization of SiR-Mito probes with MitoTracker green.

cpd.	R	M.W.	Ex/Em (nm)	Φ	clogP	Mitochondria Targeting[a]
SiR-Mito 1	2-Hydroxyl ethyl	486.3	661/668	0.32	2.29	N.D.
SiR-Mito 2	Ethyl	470.3	662/668	0.40	3.38	*
SiR-Mito 3	*n*-Butyl	498.3	652/665	0.29	4.44	-
SiR-Mito 4	Benzyl	532.3	651/666	0.30	4.82	*
SiR-Mito 5	Phenylethyl	546.3	651/669	0.29	4.95	*
SiR-Mito 6	Cyclohexylmethyl	538.3	651/668	0.30	5.50	***
SiR-Mito 7	*tert*-Octyl	554.4	650/667	0.29	5.94	***
SiR-Mito 8	Cyclooctyl	552.3	651/668	0.33	6.00	***
SiR-Mito 9	Cyclohexylethyl	552.3	652/666	0.26	6.03	***
SiR-Mito 10	2-Methylheptyl	554.4	654/667	0.27	6.33	***

[a] N.D. : not determined. */**/*** indicate the Pearson coefficient values for colocalization test between the probes and MitoTracker green. * $0.7 \leq R < 0.8$; ** $0.8 \leq R < 0.9$; *** $0.9 \leq R$

To determine the effect of probe hydrophobicity on the efficiency of targeting to mitochondria, the Pearson coefficient for colocalization of SiR-Mito probes and MitoTracker green, a commercial fluorescent mitochondrial bioprobe, was measured (**Figure 2**). For the colocalization test, human cervical cancer HeLa cells were seeded on 96-well plates and incubated for 1 h with 1 μM of each different SiR-Mito probe and 0.5 μM MitoTracker green, washed briefly with 1× PBS, and imaged with a LEICA DMi8 fluorescent microscope using the 40× objective. Interestingly, the alteration of SiR-Mito probe hydrophobicity simply based on conjugation to different amines dramatically affected mitochondria localization. Pearson coefficient values were significantly different from probe to probe, ranging from 0.01 to 0.94. For example, the incubation of HeLa cells with SiR-Mito 1, exhibiting a cLogP value below 3, resulted in the absence of fluorescence signal in the SiR channel (**Figure 2**). We concluded that fluorescent conjugates containing SiR with cLogP values lower than 3 were too polar to enter the cells. Notably, SiR-Mito probes with cLogP values between 3.38 and 4.95 (from SiR-Mito 2 to SiR-Mito 5) were associated with moderate Pearson coefficients (0.31- 0.79), whereas probes with cLogP values comprised between 5.50 and 6.33 (from SiR-Mito 6 to SiR-Mito 10) resulted in higher Pearson coefficient values (>0.9; Table 1). Therefore, the latter cLogP range appeared to be the most suitable for developing effective mitochondrial probes based on SiR fluorochromes. Notably, although the probes from SiR-Mito 6 to SiR-Mito 10 displayed similar Pearson coefficients (from 0.91 to 0.93), they exhibited different mean of intracellular fluorescence (**Figure 3**).

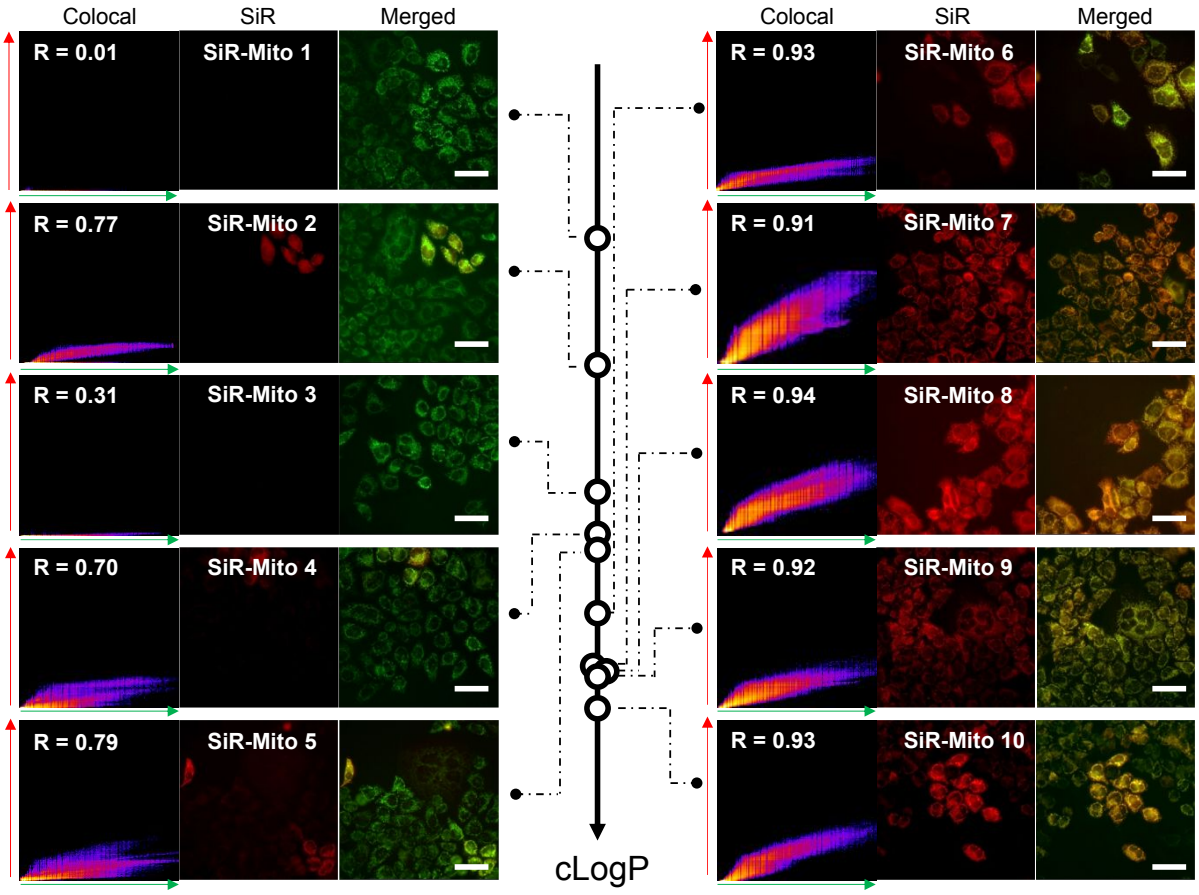

Figure 2. Colocalization test in HeLa cells stained with SiR-Mito probes and MitoTracker Red. HeLa cells were incubated with cell culture media containing 1 μM SiR-Mito probe, and 0.5 μM MitoTracker green. After 1 h, HeLa cells were washed three times with 1× PBS for and observed with a LEICA DMi8 fluorescent microscope. Each experiment was observed using 512–542 nm emitter for FITC channel (for MitoTracker Green), and 663–738 nm exciter, 545–625 nm emitter for Cy5 channel (for SiR-Mito probes). Scale bar: 50 μm.

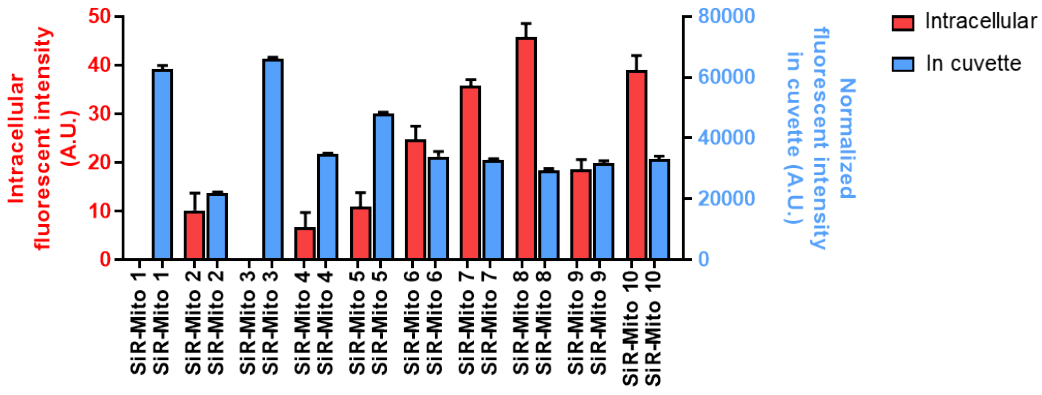

Figure 3. Fluorescent intensity comparison. Fluorescent intensity of HeLa cells incubated with equal concentrations of individual probes (Left). Normalized fluorescent intensity (Right).

The fluorescence intensities produced by equal concentrations (10^{-5} M in PBS) of the probes SiR-Mito 4 to SiR-Mito 10 were remarkably similar (**Figure 3**), demonstrating a significant impact of probe hydrophobicity on mitochondrial accumulation. Among the probes, SiR-Mito 8 exhibited the highest Pearson coefficient as well as strongest intracellular fluorescence.

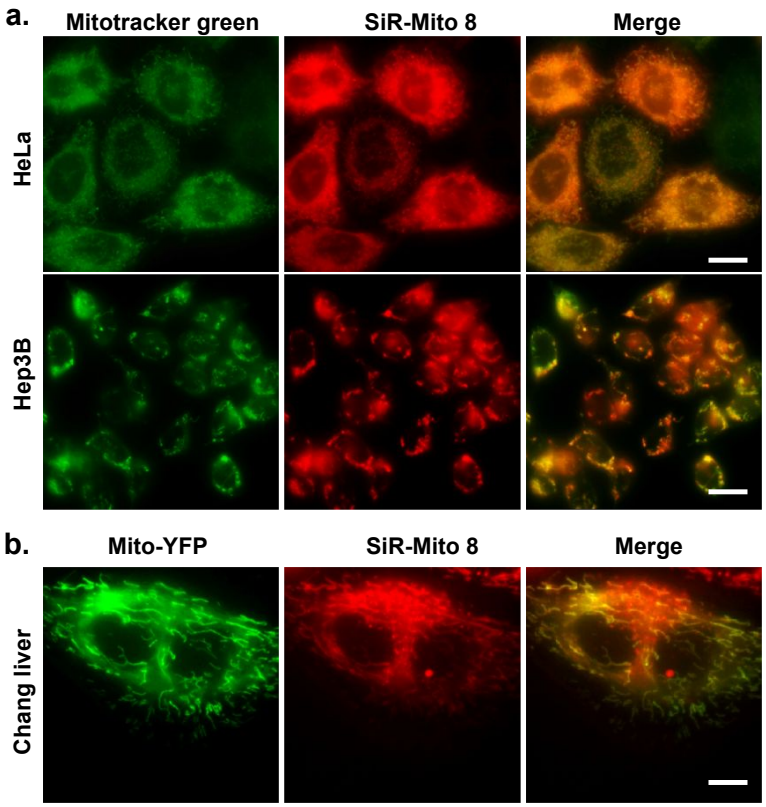

Figure 4. High resolution fluorescence imaging of mitochondria SiR-Mito 8. a) HeLa and Hep3B cells were incubated with MitoTracker Green (0.5 μM), and SiR-Mito 8 (1 μM) for 1 h. After washing 3 times with fresh media, fluorescent live cell images were acquired with LEICA DMi8 microscope. (MitoTracker green: FITC channel, SiR-Mito 8: Cy 5 channel, Scale bar: 15 μm); **b)** Chang liver cells expressing mitochondrial YFP were incubated with SiR-Mito 8 (1 μM) for 1 h. After washing 3 times with fresh media, fluorescent live cell images were acquired with LEICA DMi8 microscope. (Mitochondrial-YFP: Rhodamine channel, Scale bar: 15 μm)

High resolution imaging of HeLa and Hep3B after live cell labeling with SiR-Mito 8 and MitoTracker green shows excellent colocalization of the two probes (**Figure 4a**). In addition, high resolution imaging of Chang liver cells expressing Mitochondrial YFP (Yellow fluorescent Protein) live cell labeling with SiR-Mito 8 further confirmed high mitochondrial targeting efficiency of SiR-Mito 8 (**Figure 4b**). To verify the mitochondrial specificity of SiR-Mito 8 labeling, Hep3B human cancer cells were co-stained with a nuclear and a lysosomal tracer, in addition to SiR-Mito 8. Unlike other hydrophobic compounds, which are known to accumulate in the lysosomes of tumor cells(*22*), live cell imaging with Lysotracker Red demonstrated the high mitochondrial specificity of SiR-Mito 8 (**Figure 5**). Therefore, we focused on SiR-Mito 8 for further testing.

It is well known that the membrane potential of mitochondria is significantly higher in cancer cells than in normal cells.(*23, 24*) Therefore, we envisioned that SiR-Mito 8 could differentiate cancer cells from normal cells without involving ligand conjugation.

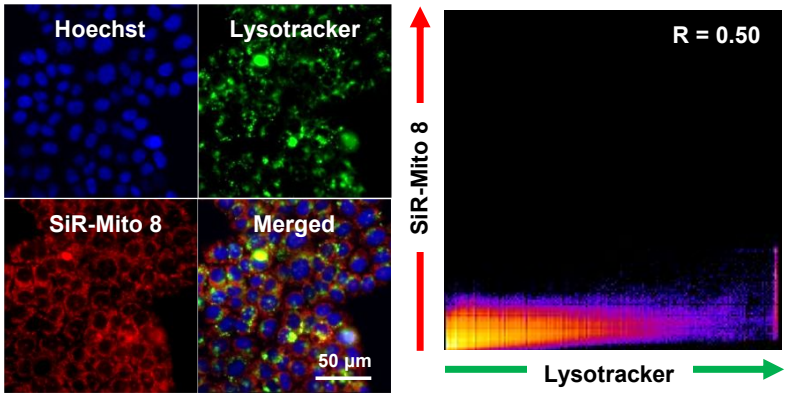

Figure 5. Co-staining with SiR-Mito 8 and Lysotracker. Liver cancer Hep3B cells were incubated with Hoechst (0.01 µg/ml), Lysotracker red (1 µM), and SiR-Mito 8 (1 µM) for 1 h. After washing 3 times with fresh media, fluorescence live cell images were acquired with a LEICA DMi8 microscope (Left). The Pearson coefficient indicates that SiR-Mito 8 did not localize to other organelle such as lysosome (Right). Scale bar: 50 µm

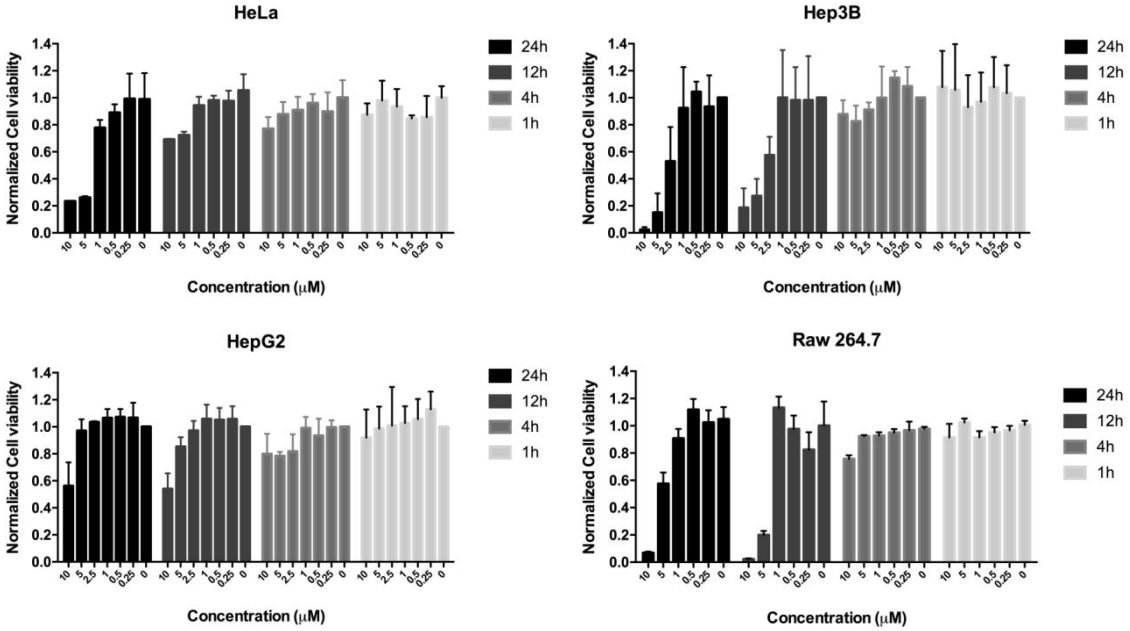

Figure 6. Cytotoxicity test. HeLa, Hep3B, HepG2 and Raw 264.7 cells were incubated with SiR-Mito 8, concentration range from 0.25 µM to 10 µM, for 1, 4, 12, and 24 h. Viability of the cells was normalized by DMSO control.

Before biological investigation of SiR-Mito 8 as a potential NIR fluorescent tracer for mitochondrial staining, cytotoxicity of the probes was evaluated. HeLa, Hep3B, HepG2 and Raw 264.7 cells were incubated with SiR-Mito 8 at various concentrations (from 0.25 to 10.0 µM) and cytotoxicity was measured by a mitochondrial respiration viability assay, confirming the lack of acute cytotoxicity by SiR-Mito 8 upto 24 h time point with moderate dose (less than 1 µM) (**Figure 6**). To demonstrate fluorescent tumor imaging, human liver cancer Hep3B cells and the human hepatocyte line, L02, were incubated with 1.0 µM SiR-Mito 8 for 1 h, washed three times with cell growth media, and imaged by a LEICA DMi8 fluorescence microscope. We found that the fluorescence intensity of the cancer cells was significantly higher (5.9 fold) than that of normal cells (**Figure 7**).

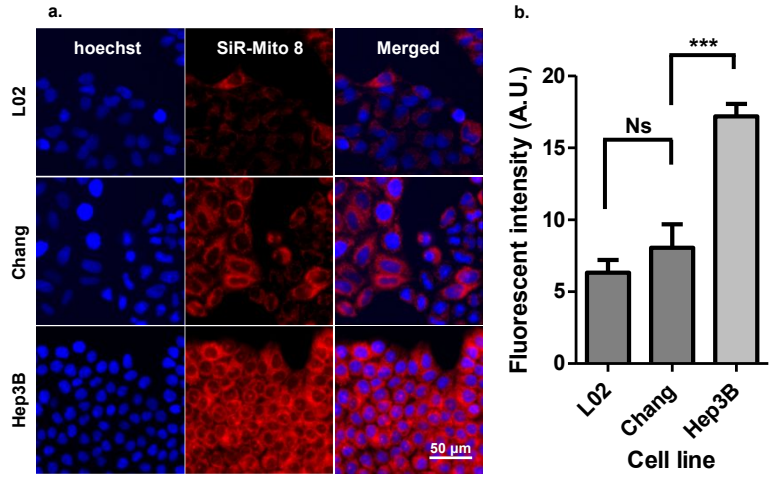

Figure 7. Cellular fluorescence images of Hep3B (liver cancer cells), L02 or Chang Liver cells (normal liver). a) Cells were incubated with full growth media containing SiR-Mito 8 (1 μM) and Hoechst dye (0.01 μg/ml) for 1 h. The cells were washed 3 times with growth media and observed with a LEICA DMi8 fluorescent microscope. Cancer cells exhibit higher fluorescence intensity than normal cells. b) Quantification of the fluorescence intensity of SiR-Mito 8 in L02, Chang liver and in Hep3B cells. Scale bar: 50 μm.

3. Conclusions

In conclusion, we have developed NIR bioprobes selectively staining mitochondria by systematic perturbation of hydrophobicity of the silicon rhodamine fluorophore. Ten different fluorescent SiR fluorochrome-based conjugates were synthesized and showed that probe hydrophobicity had a significant effect on the efficiency of mitochondria-specific staining. The optimal range of cLogP values for mitochondrial targeting by SiR fluorochromes was from 5.50 to 6.33. Among the 10 probes, SiR-Mito 8 exhibited the highest intracellular fluorescence intensity, as well as the strongest degree of colocalization with commercial fluorescent mitochondrial bioprobes in live cells. Moreover, SiR-Mito 8 was successfully applied to *in vitro* cancer-specific NIR imaging. We believe that this strategy would be useful in the future development of versatile NIR mitochondrial probes based on silicon rhodamine fluorophores. In addition, we expect that this study will inspire the usage of silicon rhodamine fluorochromes as smart drug delivery systems for theragnostics, especially for cancer.

4. Experimental Procedures

Materials and instruments

All reactions were carried out under an atmosphere of nitrogen or argon in air-dried glassware with magnetic stirring. Air- and/or moisture-sensitive liquids were transferred with syringe. Organic solutions were concentrated by rotary evaporation at 25–60 °C at 15–30 torr. All solvents and common materials were purchased from suppliers and used without further purification. Column chromatography was carried out as "Flash Chromatography" using Biotage MPLC machine. ^{1}H NMR and ^{13}C NMR data were recorded on an JEOL ECZ-600R Magnetic Resonance System (600 MHz) in Ajou University. Recorded shifts are reported in parts per million (δ): Chemical shift, multiplicity (s = singlet, d = doublet, t = triplet, q = quartet, m = multiplet,

br = broad), coupling constant (*J*, Hz) and integration. Low resolution mass spectrometry (LRMS) was obtained by LC/MS system, Finnigan MSQplus Surveyer (Thermo Scientific) or 6120 Quadrupole LC/MS (Agilent Technologies). The progress of reaction was monitored using thin layer chromatography (TLC) (silica gel 60, F254 0.25 mm), and components were visualized by observation under UV light (254 and 365 nm) or by treating the TLC plates with Phosphonolybdic acid (PMA), $KMnO_4$, or ninhydrin followed by heating. Cell culture reagents including fatal bovine serum, culture media, and antibiotic-antimycotic solution were purchased from GIBCO. MitoTracker Green, and Hoechst were purchased from Invitrogen. The culture dish and glass-bottom dish were purchased from CORNING, and SPL. All spectra experiments were performed in a 1×1 cm quartz cuvette. Fluorescence emission spectra were recorded on JASCO FP-8200 spectrofluorometer, and UV absorption spectra were recorded on JASCO V-670 spectrophotometer. Absolute quantum yield was measured by QE-2000 (Otsuka Electronics)

Chemical synthesis of SiR-Mito probes.

Synthesis of Silicon rhodamine core (compound **4**) was carried out as described in previous study(*21*).

General synthetic procedure.

A solution of compound 4 (1.0 eq), PyBOP (1.3 eq), and DIPEA (3.0 eq) in DMF was stirred for 10 min at room temperature under argon atmosphere. After 10 min, amine analog (2.0 eq) was added to reaction mixture and stirred at room temperature for overnight. Reaction mixture was directly purified with 18C reverse column chromatography with Biotage MPLC.

N-(7-(dimethylamino)-10-(5-((2-hydroxyethyl)carbamoyl)-2-methylphenyl)-5,5-dimethyldibenzo[b,e]silin-3(5H)-ylidene)-*N*-methylmethanaminium (SiR-Mito 1)

^{1}H NMR (600 MHz, Methanol-*d*4) δ 7.970 (dd, *J* =7.2Hz, 8.4Hz , 1H), 7.64 (d, *J* = 3.0 Hz, 1H), 7.54 (d, *J* = 7.8 Hz, 1H), 7.38 (d, *J* = 3.0 Hz, 2H), 7.01 (d, *J* = 9.6 Hz, 2H), 6.79 (dd, *J* = 9.0 Hz, 2H), 3.69 (t, *J* = 5.4 Hz, 2H), 3.50 (t, *J* = 5.4 Hz, 2H), 3.35 (s, 12H), 2.10 (s, 3H), 0.62, 0.61 (s, 6H); ^{13}C NMR (150 MHz, Methanol-*d*4) δ 155.8, 149.5, 142.1, 141.1, 140.4, 133.2, 131.6, 129.0, 128.8, 128.4, 122.3, 115.4, 61.5, 43.6, 40.9, 19.4, -1.2, -1.3.

N-(7-(dimethylamino)-10-(5-(ethylcarbamoyl)-2-methylphenyl)-5,5-dimethyldibenzo[b,e]silin-3(5H)-ylidene)-*N*-methylmethanaminium (SiR-Mito 2)

^{1}H NMR (600 MHz, Methanol-*d*4) δ 7.95 (dd, *J* = 7.8 Hz, 1H), 7.61 (d, *J* = 1.8 Hz, 1H), 7.53 (d, *J* = 7.8 Hz, 1H), 7.38 (d, *J* = 3Hz, 2H), 7.06 (d, *J* = 9.6 Hz, 2H), 6.79 (dd, *J* = 9.6Hz, 2H), 3.41 (t, *J* = 7.2 Hz, 2H), 3.35 (s, 12H), 2.10 (s, 3H), 1.21 (t, *J* = 6.6Hz, 3H); ^{13}C NMR (150 MHz, Methanol-*d*4) δ 169.3, 169.0, 155.8, 149.5, 142.1,

141.0, 140.4, 133.3, 131.6, 129.0, 128.7, 128.4, 122.3, 115.4, 40.9, 35.9, 19.4, 14.9, -1.2, -1.3.

N-(10-(5-(butylcarbamoyl)-2-methylphenyl)-7-(dimethylamino)-5,5-dimethyldibenzo[b,e]silin-3(5H)-ylidene)-*N*-methylmethanaminium (SiR-Mito 3)

^{1}H NMR (600 MHz, Methanol-*d*4) δ 7.95 (dd, *J* = 7.2Hz, 1H), 7.61 (d, *J* = 2.4Hz, 1H), 7.53 (d, *J* = 8.4 Hz, 1H), 7.39 (d, *J* = 2.4Hz, 2H), 7.06 (d, *J* = 9.6Hz, 2H), 6.79 (dd, *J* = 9.6Hz, 2H), 3.37 (t, *J* = 7.2 Hz, 2H), 3.35 (s, 12H), 2.10 (s, 3H), 1.59 (t, *J* = 7.2Hz, 2H), 1.40 (q, *J* = 7.8Hz, 2H), 0.96 (t, *J* = 7.8Hz, 3H), 0.62 (s, 6H); ^{13}C NMR (150 MHz, Methanol-*d*4) δ 167.9, 167.6, 154.5, 148.2, 140.8, 139.6, 139.1, 132.0, 130.3, 127.6, 127.4, 127.0, 121.0, 114.0, 39.6, 39.5, 31.3, 19.9, 18.1, 12.8, -2.5, -2.6.

N-(10-(5-(benzylcarbamoyl)-2-methylphenyl)-7-(dimethylamino)-5,5-dimethyldibenzo[b,e]silin-3(5H)-ylidene)-*N*-methylmethanaminium (SiR-Mito 4)

^{1}H NMR (600 MHz, Methanol-*d*4) δ 7.96 (dd, *J* = 8.4Hz, 1H), 7.62 (d, *J* = 2.4Hz, 1H), 7.51 (d, *J* = 8.4Hz, 1H), 7.35 (d, *J* = 3.0Hz, 2H), 7.29 (m, 5H), 7.03 (d, *J* = 3.6Hz, 2H), 6.76 (dd, *J* = 9.6Hz, 2H), 4.53 (s, 2H), 3.32 (s, 12H), 2.07 (s, 3H), 0.58 (s, 6H); ^{13}C NMR (150 MHz, Methanol-*d*4) δ 169.2, 168.9, 155.8, 149.5, 142.1, 141.2, 140.5, 140.1, 133.1 ,131.8, 129.5, 129.1, 128.8, 128.6, 128.4, 128.2, 122.3, 115.4, 44.6, 40.9, 19.5, -1.2.

N-(10-(5-((cyclohexylmethyl)carbamoyl)-2-methylphenyl)-7-(dimethylamino)-5,5-dimethyldibenzo[b,e]silin-3(5H)-ylidene)-*N*-methylmethanaminium (SiR-Mito 5)

^{1}H NMR (600 MHz, Methanol-*d*4) δ 7.95 (dd, *J* = 7.8 Hz, 1H), 7.61 (d, *J* = 2.4 Hz, 1H), 7.53 (d, *J* = 8.4 Hz, 1H), 7.38 (d, *J* = 2.4Hz, 2H), 7.06 (d, *J* = 10.2 Hz, 2H), 6.79 (dd, *J* = 9.6 Hz, 2H), 3.34 (s, 12H), 3.21 (d, *J* = 6.6 Hz, 2H), 2.10 (s, 3H), 1.76 (m, 6H), 1.28 (m, 3H), 0.99 (m, 2H), 0.62 (s, 6H); ^{13}C NMR (150 MHz, Methanol-*d*4) δ 169.3, 169.1, 155.8, 149.5, 142.1, 141.0, 140.4, 133.4, 131.6, 129.0, 128.7, 128.4, 122.3, 115.4, 47.4, 40.9, 39.3, 32.1, 27.6, 27.0, 19.5, -1.2.

N-(7-(dimethylamino)-5,5-dimethyl-10-(2-methyl-5-(phenethylcarbamoyl)phenyl)dibenzo[b,e]silin-3(5H)-ylidene)-*N*-methylmethanaminium (SiR-Mito 6)

^{1}H NMR (600 MHz, Methanol-*d*4) δ 7.90 (dd, *J* = 10.2 Hz, 1H), 7.55 (d, *J* = 2.4 Hz, 1H), 7.52 (d, *J* = 1.8 Hz, 1H), 7.38 (d, *J* = 2.4 Hz, 2H), 7.24 (m, 5H), 7.04 (d, *J* = 9.6 Hz, 2H), 6.79 (dd, *J* = 9.6 Hz, 2H), 3.58 (t, *J* = 7.8 Hz, 2H), 3.35 (s, 12H), 2.90 (t, *J* = 7.8 Hz, 2H), 2.09 (s, 3H), 0.62 (s, 6H); ^{13}C NMR (150 MHz, Methanol-*d*4) δ 167.9, 167.7, 154.5, 148.2, 140.8, 139.7, 139.2, 139.0, 132.0, 130.3, 128.5, 128.1, 127.7, 127.3, 127.0, 126.0, 121.0, 114.0, 41.3, 39.6, 35.2, 18.1, -2.5, -2.6.

N-(7-(dimethylamino)-5,5-dimethyl-10-(2-methyl-5-((2,4,4-trimethylpentan-2-yl)carbamoyl)phenyl)dibenzo[b,e]silin-3(5H)-ylidene)-*N*-methylmethanaminium (SiR-Mito 7)

^{1}H NMR (600 MHz, Methanol-*d*4) δ 7.86 (dd, *J* = 8.4 or 7.2 Hz, 1H), 7.53 (d, *J* = 1.2 Hz, 1H), 7.50 (s, 1H), 7.38 (d, *J* = 2.4 Hz, 2H), 7.05 (d, *J* = 10.2 Hz, 2H), 6.78 (dd, *J* = 10.2 Hz, 2H), 3.35 (s, 12H), 3.16 (m, 6H), 2.91 (s, 1H), 2.08 (s, 3H), 1.94 (s, 2H), 1.85 (m, 6H), 1.48 (s, 6H), 1.01 (s, 9H), 0.61, 0.60 (6H); ^{13}C NMR (150 MHz, Methanol-*d*4) δ 169.5, 168.9, 155.8, 149.6, 142.2, 140.5, 140.2, 134.9, 131.4, 129.0, 128.7, 128.4, 122.3, 115.3, 56.8, 51.2, 47.4, 47.4, 43.8, 40.9, 32.6, 31.9, 30.0, 27.4, 27.3, 19.4, -1.2.

N-(10-(5-((cyclooctylmethyl)carbamoyl)-2-methylphenyl)-7-(dimethylamino)-5,5-dimethyldibenzo[b,e]silin-3(5H)-ylidene)-*N*-methylmethanaminium (SiR-Mito 8)

^{1}H NMR (600 MHz, Methanol-*d*4) δ 7.95 (dd, *J* = 8.4 Hz, 1H), 7.60 (d, *J* = 1.8 Hz, 1H), 7.52 (d, *J* = 3.0 Hz, 1H), 7.38 (d, *J* = 3.0 Hz, 2H), 7.06 (d, *J* = 3.0 Hz, 2H), 6.79 (dd, *J* = 9.6 Hz, 2H), 4.15 (m, 1H), 3.34 (s, 12H), 2.09 (s, 3H), 1.65 (m, 13H), 0.62, 0.61 (6H); ^{13}C NMR (150 MHz, Methanol-*d*4) δ 169.4, 167.8, 155.8, 149.3, 142.2, 140.8, 140.3, 133.60, 131.5, 129.0, 128.9, 128.4, 122.3, 115.4, 51.6, 40.9, 33.4, 28.1, 26.8, 25.2, 19.4, -1.2.

N-(10-(5-((2-cyclohexylethyl)carbamoyl)-2-methylphenyl)-7-(dimethylamino)-5,5-dimethyldibenzo[b,e]silin-3(5H)-ylidene)-*N*-methylmethanaminium (SiR-Mito 9)

^{1}H NMR (600 MHz, Methanol-*d*4) δ 7.94 (dd, *J* = 7.2Hz, 1H), 7.60 (d, *J* = 1.8Hz, 1H), 7.53 (d, *J* = 7.2Hz, 1H), 7.38 (d, 3.0Hz, 2H), 7.06 (d, *J* = 9.6Hz, 2H), 6.79 (dd, *J* = 9.6Hz, 2H), 3.40 (t, *J* = 6.6 or 7.8Hz, 2H), 3.34 (s, 12H), 2.10 (s, 3H), 1.70 (m, 7H), 1.50 (d, *J* = 8.4Hz, 2H), 1.29 (m, 3H), 0.97 (m, 2H), 0.62,0.59 (6H); ^{13}C NMR (150 MHz, Methanol-*d*4) δ 168.9, 168.5, 155.4, 149.1, 141.8, 140.6, 140.0, 133.0, 131.2, 128.6, 128.3, 128.0, 121.9, 115.0, 40.5, 38.5, 37.6, 36.4, 34.0, 27.3, 27.0, 19.1, -1.6.

N-(7-(dimethylamino)-5,5-dimethyl-10-(2-methyl-5-(octan-2-ylcarbamoyl)phenyl)dibenzo[b,e]silin-3(5H)-ylidene)-*N*-methylmethanaminium (SiR-Mito 10)

^{1}H NMR (600 MHz, Methanol-*d*4) δ 8.30 (d, *J* = 8.4 Hz, 1H), 7.95 (dd, *J* = 8.4 Hz, 1H), 7.61 (d, *J* = 2.4 Hz, 1H), 7.53 (d, *J* = 2.4 Hz, 1H), 7.39 (d, *J* = 2.4 Hz, 2H), 7.07 (d, 9.6 Hz, 2H), 6.80 (dd, *J* = 9.6 Hz, 2H), 4.15 (m, 1H), 3.34 (s, 12H), 2.10 (s, 3H), 1.30 (m, 10H), 1,21 (d, *J* = 6.0 Hz, 3H), 0.87 (m, 3H), 0.62, 0.61 (6H); ^{13}C NMR (150 MHz, Methanol-*d*4) δ 169.3, 168.5, 155.9, 149.6, 142.2, 142.2, 140.9, 140.3, 133.6, 131.6, 129.0, 128.8, 128.4, 122.3, 155.4, 47.3, 40.9, 17.5, 32.9, 30.2, 27.5, 23.6, 21.0, 19.4, 14.4, -1.2, -1.3.

Cell culture and Fluorescent live cell imaging method

HeLa human cervical cancer cells were cultured in Dulbecco's modified eagle media (DMEM, GIBCO) containing 10% fetal bovine serum (FBS, GIBCO) and 1% penicillin (GIBCO) at 37 °C in a humidified incubator with 5% CO_2. For the fluorescence microscope imaging, cells were harvested using TrypLETM Express (GIBCO) and resuspended in fresh culture medium. Harvested cells with a density of 4.0×10^3 cells/well were seeded on a

96 black well plate (CORNING) and incubated for 24 h. Cells were incubated with SiR-Mito probes (1 μM) and MitoTracker Green (0.5 μM) for 60 min. After the incubation, cells were washed with 1X PBS for three times and observed with inverted fluorescence microscope (DMi8, LEICA). Each experiment was observed using a 325–375 nm exciter, 435–485 nm emitter for DAPI channel, 460–500 nm exciter, 512–542 nm emitter for FITC channel, 541-551 nm exciter, 565-605 nm emitter for Rhodamine channel, and 663–738 nm exciter, 545–625 nm emitter for Cy5 channel.

Lysotracker costaining test

6.0 x 10^4 human HCC cell line Hep3B cells were seeded on confocal dish and incubated for 2 days. After 2 days, Hep3B cells were incubated with Hoechst, 1 μM Lysotracker Red, and 1 μM SiR-Mito 8 contained media for 1 h. After the incubation, Hep3B cells were washed with cell culture media for three times and observed with inverted fluorescence microscope (DMi8, LEICA).

Fluorescent intensity comparison test between normal and cancer cell.

Hep3B, and HepG2 human liver cancer cells were cultured in Dulbecco's modified eagle media (DMEM, GIBCO) containing 10% fetal bovine serum (FBS, GIBCO) and 1% penicillin (GIBCO), and L02 human liver normal cells were cultured in Roswell Park Memorial Institute (RPMI, CAPRICORN) 1640 with L-Glutamine containing 10 % FBS (GIBCO) and 1% Penicillin (HyClone) at 37 °C in a humidified incubator with 5% CO_2. For the fluorescence microscope imaging, cells were harvested using TrypLETM Express (GIBCO) and resuspended in fresh culture medium. Harvested cells were seeded on a 96 black well plate (CORNING) with a density of 3.0 × 10^4 cells/well for cancer cells, and with a density of 4.0 x 10^4 cells/well for normal cells. After 24 h incubation. for staining of mitochondria, cells were incubated with SiR-Mito 8 (1 μM) for 60 min. Cells were washed with cell culture media for three times and observed with inverted fluorescence microscope (DMi8, LEICA).

Cytotoxicity Test

HeLa human cervical cancer cells, Hep3B and HepG2 human hepatocellular carcinoma cells, and Raw264.7 mouse macrophage cells were seeded into 96-well cell culture plates per well and allowed to adhere to the plates overnight. The cells were incubated with cell culture media containing each concentration of SiR-Mito 8 (0.25 μM to 10 μM) for 1, 4, 12 or 24h. after incubation, CellTiter 96® Aqueous One Solution Cell Proliferation Assay (Promega) was added into each well. After 2h, 490 nm absorption was measured with Cytation 3 microplate reader (BioTek). Cytotoxicity of SiR-Mito 8 was tested in triplicate in a single experiment, with each experiment being repeated at least three times.

Fluorescent high-resolution imaging in live cell

HeLa, and Hep3B cells were cultured in Dulbecco's modified eagle media (DMEM, GIBCO) containing 10% fetal bovine serum (FBS, GIBCO) and 1% penicillin (GIBCO) at 37 °C in a humidified incubator with 5% CO_2.

For the fluorescence microscope imaging, cells were harvested using TrypLETM Express (GIBCO) and resuspended in fresh culture medium. Harvested cells were seeded on a confocal dish with a density of 4.0×10^4 cells/well. After 24 h incubation, cells were incubated with SiR-Mito 8 (1 μM) and Mitotracker green (0.5 uM) for 60 min. Cells were washed three times with 1X PBS and observed with inverted fluorescence microscope (DMi8, LEICA).

Plasmid transfection.

Overexpression plasmid for Mitochondria-YFP was obtained from Catholic University (Seoul, Korea) and transfected into Chang liver cells. Stable clones expressing Mitochondria-YFP was selected using 0.25mg/ml G418.

Costaining test of SiR-Mito 8 with Mitochondria-YFP

Mitochondria-YFP infected Chang liver cells were cultured in Dulbecco's modified eagle media (DMEM, GIBCO) containing 10% fetal bovine serum (FBS, GIBCO) and 1% penicillin (GIBCO) at 37 °C in a humidified incubator with 5% CO_2. For the fluorescence microscope imaging, cells were harvested using TrypLETM Express (GIBCO) and resuspended in fresh culture medium. Harvested cells were seeded on a confocal dish with a density of 4.0×10^4 cells/well. After 24 h incubation, cells were incubated with SiR-Mito 8 (1 μM) for 60 min. Cells were washed three times with 1X PBS and observed with inverted fluorescence microscope (DMi8, LEICA).

Notes

The authors declare no competing financial and non-financial interests.

Supporting Information

^{1}H NMR spectrums, ^{13}C NMR spectrums, abs spectrums and emission spectrums of SiR-Mito probes.

Acknowledgments

This work was supported by Basic Research Program (2009-0093826, 2016R1E1A1A01941213 and 2016R1C1B2014699) through the National Research Foundation of Korea (NRF) funded by the Korean Government (Ministry of Science and ICT) and by the Ajou University research fund.

References

(1) Murphy, Michael P. (2009) How mitochondria produce reactive oxygen species. *Biochemical Journal 417*, 1-13.
(2) Green, D. R., and Reed, J. C. (1998) Mitochondria and Apoptosis. *Science 281*, 1309-1312.
(3) Willems, P. H., Rossignol, R., Dieteren, C. E., Murphy, M. P., and Koopman, W. J. (2015) Redox Homeostasis and Mitochondrial Dynamics. *Cell Metab 22*, 207-18.
(4) West, A. P., Shadel, G. S., and Ghosh, S. (2011) Mitochondria in innate immune responses. *Nature*

Reviews Immunology 11, 389.
(5) Green, D. R., Galluzzi, L., and Kroemer, G. (2011) Mitochondria and the Autophagy–Inflammation–Cell Death Axis in Organismal Aging. *Science 333*, 1109-1112.
(6) Beal, M. F. (1998) Mitochondrial dysfunction in neurodegenerative diseases. *Biochimica et Biophysica Acta (BBA) - Bioenergetics 1366*, 211-223.
(7) Madamanchi, N. R., and Runge, M. S. (2007) Mitochondrial dysfunction in atherosclerosis. *Circ Res 100*, 460-73.
(8) Lowell, B. B., and Shulman, G. I. (2005) Mitochondrial Dysfunction and Type 2 Diabetes. *Science 307*, 384-387.
(9) Youle, R. J., and van der Bliek, A. M. (2012) Mitochondrial Fission, Fusion, and Stress. *Science 337*, 1062-1065.
(10) Westermann, B. (2010) Mitochondrial fusion and fission in cell life and death. *Nature Reviews Molecular Cell Biology 11*, 872.
(11) Westermann, B. (2012) Bioenergetic role of mitochondrial fusion and fission. *Biochimica et Biophysica Acta (BBA) - Bioenergetics 1817*, 1833-1838.
(12) Giedt, R. J., Fumene Feruglio, P., Pathania, D., Yang, K. S., Kilcoyne, A., Vinegoni, C., Mitchison, T. J., and Weissleder, R. (2016) Computational imaging reveals mitochondrial morphology as a biomarker of cancer phenotype and drug response. *Scientific Reports 6*, 32985.
(13) Zielonka, J., Joseph, J., Sikora, A., Hardy, M., Ouari, O., Vasquez-Vivar, J., Cheng, G., Lopez, M., and Kalyanaraman, B. (2017) Mitochondria-Targeted Triphenylphosphonium-Based Compounds: Syntheses, Mechanisms of Action, and Therapeutic and Diagnostic Applications. *Chemical Reviews 117*, 10043-10120.
(14) Murphy, M. P. (2008) Targeting lipophilic cations to mitochondria. *Biochimica et Biophysica Acta (BBA) - Bioenergetics 1777*, 1028-1031.
(15) Murphy, M. P., and Smith, R. A. J. (2000) Drug delivery to mitochondria: the key to mitochondrial medicine. *Advanced Drug Delivery Reviews 41*, 235-250.
(16) Smith, R. A. J., Hartley, R. C., and Murphy, M. P. (2011) Mitochondria-Targeted Small Molecule Therapeutics and Probes. *Antioxidants & Redox Signaling 15*, 3021-3038.
(17) Lei, E. K., and Kelley, S. O. (2017) Delivery and Release of Small-Molecule Probes in Mitochondria Using Traceless Linkers. *Journal of the American Chemical Society 139*, 9455-9458.
(18) Fu, M., Xiao, Y., Qian, X., Zhao, D., and Xu, Y. (2008) A design concept of long-wavelength fluorescent analogs of rhodamine dyes: replacement of oxygen with silicon atom. *Chem Commun (Camb)*, 1780-2.
(19) Koide, Y., Urano, Y., Hanaoka, K., Terai, T., and Nagano, T. (2011) Evolution of Group 14 Rhodamines as Platforms for Near-Infrared Fluorescence Probes Utilizing Photoinduced Electron Transfer. *ACS Chemical Biology 6*, 600-608.
(20) Lukinavičius, G., Umezawa, K., Olivier, N., Honigmann, A., Yang, G., Plass, T., Mueller, V., Reymond, L., Corrêa Jr, I. R., Luo, Z.-G., Schultz, C., Lemke, E. A., Heppenstall, P., Eggeling, C., Manley, S., and Johnsson, K. (2013) A near-infrared fluorophore for live-cell super-resolution microscopy of cellular proteins. *Nature Chemistry 5*, 132.
(21) Kim, E., Yang, K. S., Giedt, R. J., and Weissleder, R. (2014) Red Si-rhodamine drug conjugates enable imaging in GFP cells. *Chem Commun (Camb) 50*, 4504-7.
(22) Dahal, D., McDonald, L., Bi, X., Abeywickrama, C., Gombedza, F., Konopka, M., Paruchuri, S., and Pang, Y. (2017) An NIR-emitting lysosome-targeting probe with large Stokes shift via coupling cyanine and excited-state intramolecular proton transfer. *Chem Commun (Camb) 53*, 3697-3700.
(23) Summerhayes, I. C., Lampidis, T. J., Bernal, S. D., Nadakavukaren, J. J., Nadakavukaren, K. K., Shepherd, E. L., and Chen, L. B. (1982) Unusual retention of rhodamine 123 by mitochondria in muscle and carcinoma cells. *Proceedings of the National Academy of Sciences 79*, 5292-5296.
(24) Davis, S., Weiss, M. J., Wong, J. R., Lampidis, T. J., and Chen, L. B. (1985) Mitochondrial and plasma membrane potentials cause unusual accumulation and retention of rhodamine 123 by human breast adenocarcinoma-derived MCF-7 cells. *Journal of Biological Chemistry 260*, 13844-50.

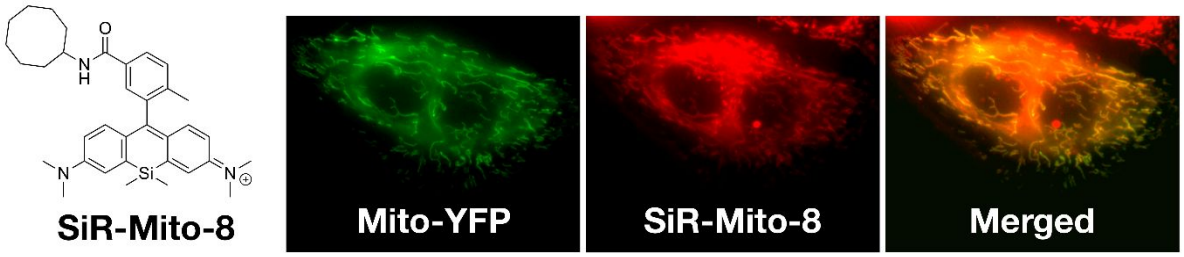

graphic table of contents